Quorum sensing digital simulations for the emergence of scalable and cooperative artificial networks

Nedjma Djezzar, Iñaki Fernández Pérez, Nouredinne Djedi, Yves Duthen

▶ **To cite this version:**

Nedjma Djezzar, Iñaki Fernández Pérez, Nouredinne Djedi, Yves Duthen. Quorum sensing digital simulations for the emergence of scalable and cooperative artificial networks. International Journal of Artificial Intelligence and Machine Learning, 2019, 9 (1), pp.13-34. 10.4018/IJAIML.2019010102 . hal-03462954

HAL Id: hal-03462954
https://hal.science/hal-03462954

Submitted on 2 Dec 2021

HAL is a multi-disciplinary open access archive for the deposit and dissemination of scientific research documents, whether they are published or not. The documents may come from teaching and research institutions in France or abroad, or from public or private research centers.

L'archive ouverte pluridisciplinaire **HAL**, est destinée au dépôt et à la diffusion de documents scientifiques de niveau recherche, publiés ou non, émanant des établissements d'enseignement et de recherche français ou étrangers, des laboratoires publics ou privés.

Open Archive Toulouse Archive Ouverte

OATAO is an open access repository that collects the work of Toulouse researchers and makes it freely available over the web where possible

This is an author's version published in:
http://oatao.univ-toulouse.fr/26314

Official URL

https://doi.org/10.4018/IJAIML.2019010102

To cite this version: Djezzar, Nedjma and Fernández Pérez, Inaki and Djedi, Nouredinne and Duthen, Yves *Quorum sensing digital simulations for the emergence of scalable and cooperative artificial networks.* (2019) International Journal of Artificial Intelligence and Machine Learning, 9 (1). 13-34. ISSN 2642-1577

Any correspondence concerning this service should be sent to the repository administrator: tech-oatao@listes-diff.inp-toulouse.fr

Quorum Sensing Digital Simulations for the Emergence of Scalable and Cooperative Artificial Networks

Nedjma Djezzar, LESIA-Biskra University / IRIT- Université Toulouse 1 Capitole, Toulouse, France
Iñaki Fernández Pérez, IRIT- Université Toulouse 1 Capitole, Toulouse, France
Noureddine Djedi, LESIA laboratory, Biskra University, Biskra, Algeria
Yves Duthen, IRIT- Université Toulouse 1 Capitole, Toulouse, France

ABSTRACT

This article proposes digital simulations of a bacterial communication system termed quorum sensing, and investigates the design of artificial networks build on the behavior of bacteria societies that tweet using quorum sensing signals. To this end, this article proposes a cell-based model that uses a "bottom-up" agent-based model coupled with ordinary differential equations, and develops the abstraction of intracellular dynamics as a basis underlying cooperative artificial network formation. Results show the emergence of self-sustainable behaviors thanks to the proposed model of metabolism that permits bacteria to grow, reproduce, interact, and coordinate at the population level to exhibit near-perfect bioluminescence behaviors. Moreover, the evolution of cooperation in the subsequent artificial network leads to the emergence of non-predicted coercive strategies. Coercion has been shown to be beneficial to share common interests between variants of cooperators leading the entire population of cells to be networked.

KEYWORDS

Agent-Based Modeling, Autonomous Behavior, Bioluminescence, Cell-to-Cell Communication, Coercion, Cooperation, Distributed Control, Gene Expression, Metabolism, Self-Regulation

INTRODUCTION

The simulation and design of biological mechanisms of self-regulation has been shown to provide insights through engineering digital artefacts that display self-organized, scalable and robust features which is one of the key purposes of the artificial life research. One of the self-organizing mechanisms of biological systems is that their units have the ability to communicate to help to fulfill their goals. For instance, there is a growing realization that the robustness of biological systems is often derived from collective population-level behaviors that extend beyond individual cells (Gorochowski, 2016). In the context of unicellular organisms, bacteria were for a long time thought to be independent unicellular organisms, until 1979, when bacterial colonies of Gram-negative bacteria such as Vibrio-fischeri

DOI: 10.4018/IJAIML.2019010102

and Vibrio-harveyi were shown to be able to perform a collective light-emitting behavior (Bassler, 1999). Traditionally, this phenomenon is known as Quorum Sensing (QS), and happens when the cellular density reaches a certain threshold. Indeed, bacteria cells can communicate with each other by producing, realizing, and taking up diffusible signaling molecules known as "autoinducers". When the autoinducer bounds to the target genetic receptor in a receiving cell, this results in the production of more signaling molecules. At high cell densities, this process causes the triggering of specific phenotypic responses such as bioluminescence or biofilm formation.

Communication is a widespread phenomenon in natural organisms and is fundamental to any kind of coordinated, parallel and distributed processes in human designed systems. The design and simulation of cellular communications has been explored by the artificial life community in two backgrounds: multicellular (Doursat, Sayama, & Michel, 2013; Stanley & Miikkulainen, 2003) and unicellular organisms. However, cell signaling in unicellular organisms is less studied. Indeed, there are fewer works on cell signaling in unicellular cell signaling.

We believe that the unicellular approach, provides several intrinsic beneficial properties, e.g. all the organisms are autonomous and share a single distributed communication system (QS). In addition, despite their sizes, single celled organisms such as bacteria have computational and evolutionary autonomous capabilities for self-replication and self-organization (Majumdar & Mondal, 2016). Moreover, an improved understanding of unicellular signaling by QS has numerous scientific benefits (Beckmann & Mckinley, 2009) and may provide insight into the evolution of multicellularity itself. Indeed, compared to a cell from a multicellular organism, a bacterial cell is a mobile and autonomous entity that can grow and act independently at an individual level, and coordinate its behavior with other cells at a population level to exhibit coordinated features previously recognized as specific to multicellular organisms, e.g. shape formation (Pascalie et al., 2016).

The potential of QS then resides in the simplicity of its general concept that gives rise to complex behaviors. But it should be noted that, although QS is simple in its fundamental principles, the QS mechanism is complex in its biological details. Although we have a good understanding of intra-cellular mechanisms, there remains considerable challenges.

We believe that abstracting the complex interactions of cell-to-cell communication into a representation will enrich our understanding of complex bacterial societies and may provide insights for alternative design techniques.

Thus, this paper proposes a multiagent computational model of QS, and investigates the potential of the link that can be established between QS and artificial communication networks. Specifically, the model uses a bottom-up agent-based approach and proposes a cell-based model coupled with Ordinary Differential Equations (ODEs) that abstract the intracellular dynamics of a bacterium cell such as a model of growth, a model of communication, a model of light - production, and a model of metabolism.

Our model is tested in a set of experiments (Djezzar, Fernandez Perez, Djedi, & Duthen, n.d.) where we evaluate the communication capabilities of bacterial colonies, their self-organized bioluminescence behavior, and their sustainable abilities to cooperatively form artificial communication networks. Results show evolution of cooperation and emergence of coercive strategies.

Our bacterial-inspired networks could be potentially used for the emergence of robust and autonomous network topologies that can address issues such as mobility or energy, which are key factors for the development of new self-organizing networks (Aziz, Sekercioglu, Fitzpatrick, & Ivanovich, 2013; Dressler & Akan, 2010).

The rest of this paper is organized as follows. Section 2 presents the related works and the problem statement. Our cellular model and their main parts, explicitly: growth, quorum sensing, metabolism and light-production, are detailed in Section 3. The proposed artificial communication network model is presented in section 4. Simulations results are evaluated and discussed in section 5 and 6. Section 7 outlines the model parameters and Section 9 concludes the paper.

BACKGROUND AND PROBLEM STATEMENT

Given its relevance as a simple and powerful biological communication system, QS has attracted the interest of interdisciplinary research groups. In the field of bioinspired systems, QS has been investigated from various perspectives, including: membrane computing (Esmaeili & Yazdanbod, 2009; Romero-Campero & Pérez-Jiménez, 2008), decision-making in mobile autonomous team (Sofge & Lawless, 2011), nanomachine computing (Wiedermann, 2011), logic computing (Ji et al., 2013), dynamic clustering (Tan & Slotine, 2013), agent-based modeling (Niu, Wang, Duan, & Li, 2013), artificial ecosystems (Beckmann & Mckinley, 2009; Ouannes, Djedi, Duthen, & Luga, 2016), game theory (Burgos & Polani, 2016), as well as, nanoscale robotic cooperation (Amir, Abu-Horowitz, Werfel, & Bachelet, 2018; Q. Zhao, Li, Wang, Li, & Luo, 2015), and humanoid robot synchronization (Bechon & Slotine, 2012).

Moreover, many mathematical models have proposed the simulation of phenotypic traits of QS particularly biofilm formation (Emerenini, Hense, Kuttler, & Eberl, 2015; J. Zhao & Wang, 2017).

In the field of artificial life, few works have investigated digital simulations of QS considering metabolism and bioluminescence. While in the seminal works of (J. W. Williams, Cui, Levchenko, & Stevens, 2008) and (Melke, Sahlin, Levchenko, & Jönsson, 2010), a QS simulation was proposed, their model did not consider bacterial metabolism for energy production and consumption. Since energy is vital to any physiological process in living organisms, that model of metabolism is included in our simulations. Further, we propose a computational model of bioluminescence using the same QS model, and the same environment shared by cells. Such light-producing behaviors in natural cells have attracted a growing interest in the research community. Indeed, researchers have investigated the possibility of using bioluminescent systems for bio-lightning and as a concrete example, a bioluminescent plant has been developed (Callaway, 2013). More recently and from a more abstract perspective, Song and Yamada (Song & Yamada, 2018) have proposed a bioluminescence-inspired model for the simulation of human-robot interaction. In our model we use bioluminescence as a basis underlying the cooperative formation of artificial communication networks.

On the other hand, few works have investigated the analogy between QS and communication networks. In our work, we establish a conceptual link between QS and artificial communication networks. In (Wei, Walsh, Cazan, & Marculescu, 2015), a QS-based communication network model was proposed, which used autoinducer molecules for communication. In our work, we address a similar problem using a network-centric approach, but we use a light-based communication protocol instead of autoinducers, because the propagation of light is less limited by distance than a signaling molecule. Moreover, the variance in the light intensities is favorable for cluster-based structures by providing hierarchical cell types: super-spreaders of light called wild-type cooperators, simple spreaders called cooperators and non-spreaders of light called cheaters. Hierarchical structures are recognized to be beneficial for the optimization of the network resources such as energy (Aziz et al., 2013).

CELLULAR DYNAMICS MODEL

Cells are mobile agents that evolve in a 2D environment and have the ability of sensing the environment (taking up substrates and autoinducers), growing, dividing and surviving. They possess a QS genetic controller circuit allowing them to coordinate their cellular communication with other cells. Moreover, they can synthesize light via a proposed model of bioluminescence and have a metabolism allowing them to accomplish all of these actions.

Growth

Cell growth is the primary response of viable cells to substrates and nutrients. It occurs *via* a growth of the cell mass followed by a cell division (Figure 1). For simplicity, in our model, the cell mass grow through the Monod limiting-substrate growth model (Monod, 1949). We use a substrate-limited

Figure 1. Cell growth kinetics using Monod model (Monod, 1949). An increase of the cell mass followed by cell division.

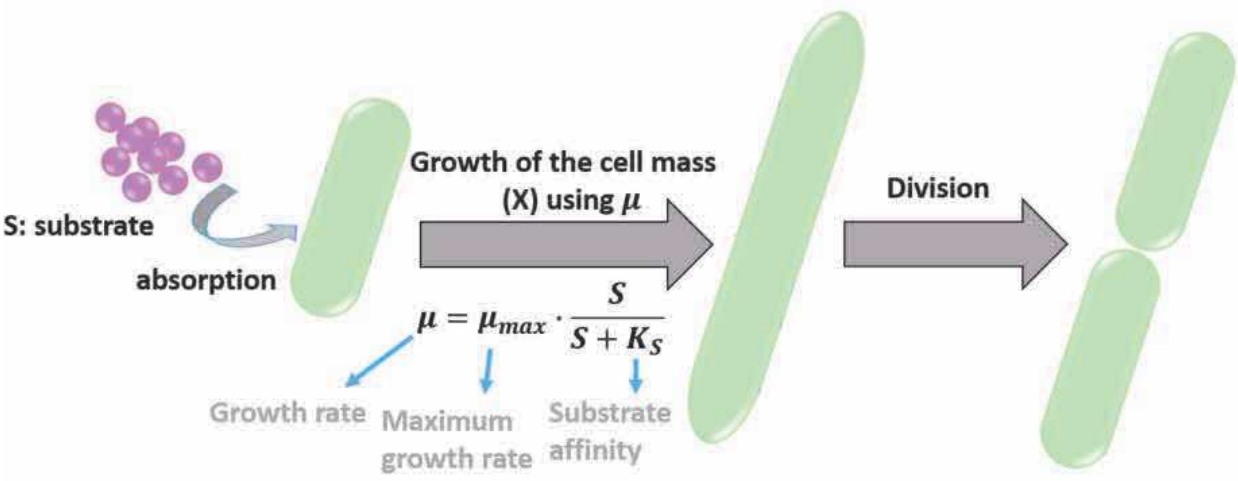

model because it is generally observed that the substrate and energy (ATP) consumption rates are higher under substrate-sufficient conditions than under substrate limitation conditions (Zeng & Deckwer, 1995). In Monod model, the specific growth rate $\left(\mu\right)$ of a bacterium biomass $\left(X\right)$ depends on the substrate concentration $\left(S\right)$. The equation is given by:

$$\mu = \mu_{max} \cdot \frac{S}{S + K_S} \tag{1}$$

where μ_{max} is the maximum growth rate and k_s is the substrate affinity (the value of S when $\mu / \mu max = 0.5$). These two parameters are assumed to be constant, but depend on strain and environmental conditions. Using the specific growth rate $\left(\mu\right)$, $d\left[X\right] / dt$ is calculated as follows:

$$\frac{d\left[X\right]}{dt} = X \cdot \mu \tag{2}$$

As a cell takes up substrates, it grows until it doubles size, at which point it divides. When the cell divides, it gives rise to two cells. One of the cells is arbitrarily chosen to be the mother and the other the daughter. Then, the program running on the mother is copied, and the copy is associated with the daughter.

To calculate the specific energy requirement rate $\left(q_{ATP}\right)$ for cell growth, we use the energetic growth yield coefficients $\left(Y_{X/ATP}\right)$. This parameter is assumed to be constant and represents the cell mass synthesized $\left(X\right)$ per a unit of energy generated (ATP). The equation is given by:

$$q_{ATP} = \frac{\mu}{Y_{X/ATP}} \tag{3}$$

Note that the energy (ATP) consumption due to the cell growth is subtracted from the total energy of the cell.

Cell-to-Cell Communication

To simulate cell-to-cell communication in heterogeneous microbial communities, we use a generic LuxI / LuxR QS language that is employed by over 30 species of Gram-negative bacteria (Bassler, 1999). All LuxI / R systems are mediated by autoinducers, such as acylated homoserine lactone (AHL). Typically, the process involves bacterial cells releasing small diffusible signals (AHL molecules). Cells respond to the uptake of the AHL molecules by producing more AHL molecules. At low cell densities, cells produce only a basal level of AHL, so there is only a low concentration in the environment. When the cell density starts increasing, then, there will be higher levels of AHL, causing the activation of specific genes in the genome. There are specific genes for each specific phenotype: bioluminescence, biofilm, etc.

Our computational model of the molecular regulation network is based on the empirical ODE-models proposed by (J. W. Williams et al., 2008) and (Melke et al., 2010). This model uses two positive feedback loops as illustrated in Figure 2. The AHL molecule (A) and the receptor LuxR (R) form a complex (RA). Two molecules of the complex (RA) form the dimerized complex (C). The dimerized complex (C) regulates the expression of both:

- luxI genes which produce more, AHL molecules (positive feedback loop1); and
- luxR genes which produce more LuxR receptors (positive feedback loop 2).

Figure 2. The molecular regulation process of the *LuxI/LuxR* quorum sensing. The paradigm for *LuxI/LuxR* QS systems consists of two proteins: LuxI produces the autoinducer (AHL) molecules, and LuxR is responsible for detecting these molecules. When the AHL bonds to the LuxR receptor, a LuxR-AHL complex is then created. The dimerized complex composed of two molecules of LuxR-AHL complex activates two things: 1) the transcription of LuxI (positive feedback loop 1, and 2) the transcription of LuxR (positive feedback loop 2), which results in the production of more AHL molecules and LuxR receptors. At high cell densities the process leads to the activation of specific genes in the genome such as luminescence genes.

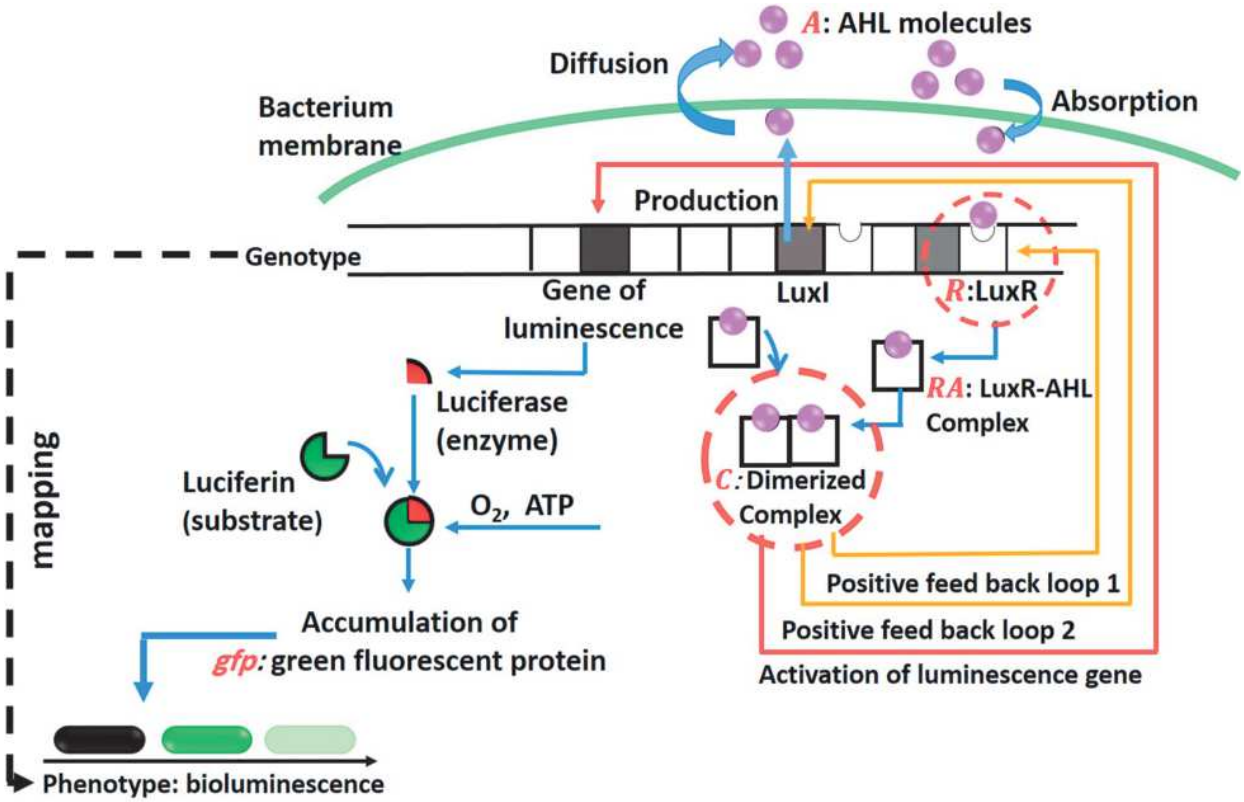

The corresponding equations are described as follows:

$$\frac{d[A]}{dt} = C_A + \frac{k_A[C]}{K_A + [C]} - k_0[A] - k_1[R][A] + k_2[RA] - p_e[A] + p_a[A_e] \tag{4}$$

$$\frac{d[R]}{dt} = C_R + \frac{k_R[C]}{K_R + [C]} - k_3[R] - k_1[R][A] + k_2[RA] \tag{5}$$

$$\frac{d[RA]}{dt} = k_1[R][A] - k_2[RA] - 2k_4[RA]^2 + 2k_5[C] \tag{6}$$

$$\frac{d[C]}{dt} = k_4[RA]^2 - k_5[C] \tag{7}$$

$$\frac{d[A_e]}{dt} = \sum_{bact}\left(p_e[A] - p_a[A_e]\right) + D\nabla^2[A_e] \tag{8}$$

where the notation $[X]$ represents the concentration of a molecular species X. C_A and C_R represent the basal level transcription of A and R, respectively. A_e is the extracellular concentration of A in the environment. p_e and p_a are emission and absorption rates of A and A_e respectively. The constant parameters values are listed in Table 2 in the model parameter Section.

Light Production

In general, light production usually known as bioluminescence or photogenesis is a chemical reaction catalyzed by a photoprotein enzyme called luciferase. The luciferase is responsible for transforming a light-producing substrate called luciferin into light. The process requires the presence of other substances, like oxygen and adenosine triphosphate (ATP). For simplicity, oxygen is assumed to exist in abundance in the environment. The enzymatic reaction can therefore be written in the form of a bi-molecular reaction that involves an enzyme (E), binding to a substrate (S) to form a complex (ES), which in turn releases a product (P), regenerating the original enzyme. This may be represented as follows:

$$E + S \underset{K_r}{\overset{K_f}{\leftarrow\!\!\rightarrow}} ES \overset{K_{cat}}{\rightarrow} E + P \tag{9}$$

where K_f is the forward rate, K_r the reverse rate, and K_{cat} the catalytic rate. By applying conservation constraints of the material and assuming that the concentration of enzymes is very low in comparison to the metabolite concentration, the equation describing this reaction is resolved to:

$$\frac{d[P]}{dt} = \frac{K_{cat}[E][S]}{\frac{K_r + K_{cat}}{K_f} + [S]} \tag{10}$$

By setting:

$$K_L = \frac{K_r + K_{cat}}{K_f} \text{ and } P_{max} = K_{cat}[E]$$

we obtain the following equation:

$$\frac{d[P]}{dt} = \frac{P_{max}[S]}{K_L + [S]} \tag{11}$$

where P_{max} represents the maximum production rate and K_L is the concentration of S where the reaction rate is half-maximum.

In the case of bioluminescent bacteria, the bacterial luciferase is encoded and synthesized by the lux operon. The transcription of the lux operon is activated by the LuxR - AHL dimerized complex (C), as shown in Figure 2. The bacterium produces light only at high cell density. More precisely, when a quorum is reached. At low cell densities, even with higher concentrations of the luciferin substrate, bacteria cells do not produce light. Then, we assume that: (1) the substrate exists abundantly in the cell cytoplasm and (2) the dimerized complex C that controls the synthesis of the luciferase enzyme is assumed to be a determining factor. We therefore model light production as a function of the dimerized complex C, hence Equation 11 is modified to:

$$\frac{d[L]}{dt} = \frac{L_{max}[C]}{K_L + [C]} \tag{12}$$

where L is the light production rate, L_{max} the maximum light production rate, and K_L the concentration of C where L is at half-maximum. Bioluminescence is expressed as the accumulation of the green fluorescent protein gfp. The gfp is incremented at each time step according to the light production rate L.

Metabolism

Metabolism is calculated as the organism total energy. The sum of basal energy and substrate energy from which the energy spent to grow, divide, produce light, or simply survive (maintenance energy) is subtracted. Figure 3 represents material and energy inputs and outputs of the bacterium metabolism. Since ATP is the molecule that stores and transports energy in living organisms, we model the bacterial ATP cycle as follows:

$$\Delta ATP = \left(ATP_0 + E.ATP_S + ATP_G + ATP_D + ATP_L + ATP_M\right)\left(\Delta t\right) \tag{13}$$

Figure 3. The model of bacterial metabolism. Energy and material inputs and outputs.

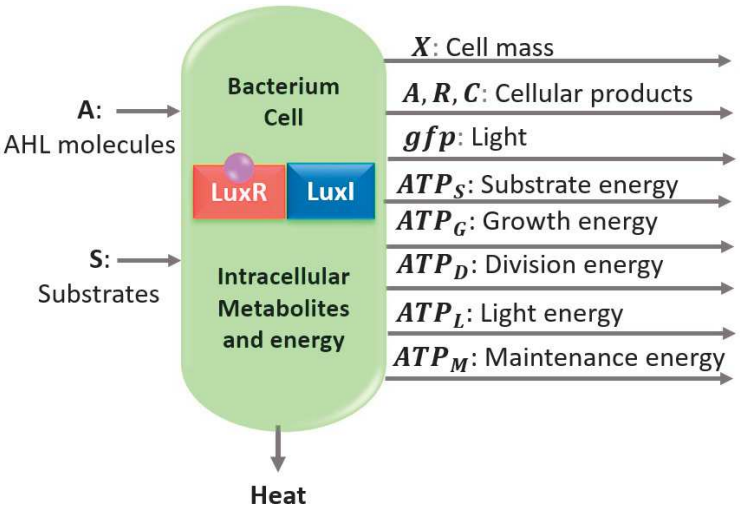

where:

- ΔATP is the total organism energy expenditure;
- ATP_0 is the basal energy;
- ATP_S is the substrate energy. It represents the energy produced from metabolized substrates. This term is calculated as follows:

$$\frac{d\left[ATP_S\right]}{dt} = Y_{ATP/S} \cdot \frac{d\left[S\right]}{dt} \tag{14}$$

where $Y_{ATP/S}$ is the energetic substrate yield. It represents the amount of ATP produced per a unit of substrate:

- E is the substrate metabolism efficiency (equal to 40%) as only 40 to 50% of the energy stored in a carbon substrate is converted to biological energy (ATP). The rest is released as heat (Figure 3);
- ATP_G is the growth energy. It represents the energy consumption due to the cell growth. The consumption of ATP due to the cell growth, at each time step, is given by:

$$\frac{d\left[ATP_G\right]}{dt} = -q_{ATP} \cdot X \tag{15}$$

Using Equation 3, Equation 15 becomes:

$$\frac{d\left[ATP_G\right]}{dt} = -\frac{\mu}{Y_{X/ATP}} \cdot X \tag{16}$$

Using Equation 2, Equation 16 becomes:

$$\frac{d\left[ATP_G\right]}{dt} = -\frac{1}{Y_{X/ATP}} \cdot \frac{d\left[X\right]}{dt} \tag{17}$$

- ATP_D is the division energy. It represents the energetic cost of cell division and is equal to 0.5 μM ;
- ATP_L is the light energy. It represents the energy used to produce light. We use a similar equation in Equation 17 to calculate ATP_L . This is given by:

$$\frac{d\left[ATP_L\right]}{dt} = -\frac{1}{Y_{L/ATP}} \cdot \frac{d\left[L\right]}{dt} \tag{18}$$

where $Y_{L/ATP}$ is the energetic light yield coefficient.

- ATP_M is the maintenance energy (equal to 0.25 μM).

LIGHT-BASED ARTIFICIAL NETWORK

The QS-based communication network differs from a classical network due to the fact that bacteria cells do not have IP addresses and the signals that they convey do not have specific destinations. Consequently, the information coded in the signals cannot be precisely "routed" to the target receiver in the network. However, the QS-based communication network is similar to traditional computer networks in several aspects:

- Traditional networks can connect heterogeneous devices. Within microbiomes, different types of bacteria can establish molecular communication networks;
- The strength of the emitted signal may be analogous to the light intensity;
- The sensitivity of the receiver is analogous to the concentration of the signal receptor $\left(Lux\ R\right)$.

Network Links

Based on the above observations, we propose a QS network definition based only on intracellular factors. Specifically, a directed link is established from bacterium A to bacterium B under two conditions:

- The light signal concentration $\left(gfp\ /\ volume\right)$ inside bacterium A is larger than that of bacterium B;
- A bacterium B is a sensitive receiver to light if its concentration of $LuxR$ is above an activation threshold TR.

The first condition specifies the link direction. It represents the fact that there is a descending light gradient from bacterium A to Bacterium B. the second condition ensures that bacterium B can receive the signal.

Network Nodes

A node is an abstraction of a bacterium cell. As within microbiomes, different types of cooperators and cheaters (not producers) tend to coexist in collaboration or in conflict (Moreno-Fenoll, Cavaliere,

Martínez-García, & Poyatos, 2017; Sexton & Schuster, 2017), we adopt a similar biological terminology to define the node's type of our communication network.

To account for different light productivity, we classify the network nodes into three categories based on the intracellular intensity of light (Figure 4). More precisely, nodes with $\mathrm{gfp} / \mathrm{volume} > 20$ are up-regulated cells with high light productivity. This category of nodes is a super spreader that can send light to all the other types of node. They are considered to be wild-type cooperators (WT cooperators). Nodes with $0 < gfp / volume < 20$ are considered to be cooperators. These nodes are down-regulated cells that can receive light from all WT cooperators, but do not produce light at high

intensity. So, they are able to send light to sensitive cheater cells at a rate equal to $\mathrm{T_L} = 0,20$. Finally, cheater nodes are non-bioluminescent bacteria with $\mathrm{gfp} / \mathrm{volume} = 0$. They may be non-QS cells or QS cells that do not produce light. They are receivers called cheaters because they do not collaborate toward the common interests (establishing links via sending light) but gain benefit from those that do.

EXPERIMENTS AND RESULTS

Using an open source simulator (Jang, Oishi, Egbert, & Klavins, 2012), we set up a 2D environment of size $\left(80\,\mu m, 80\,\mu m\right)$. At the beginning of the simulation, 100 generic bacterial agents were randomly dispersed in the environment (Figure 5a). A bacterium cell is assumed to be $1\mu m$ in diameter and, initially *2 μm* long. So that, its initial volume is $V = 1.57 fl$ (femtoliters). To support the survival and growth of bacteria cells, a constant substrate concentration $S = 10\,\mu Mol$ is assumed. As a cell takes up substrates, it grows until it doubles in volume to $V = 3.14 fL$, at which point it divides.

Quorum Sensing

The quorum is met at $\mathrm{t} \simeq 180\ \mathrm{min}$, when the population size is 250 cell (Figure 5d). From t = 270 min (Figure 5g- h), we can clearly see the AHL in blue around the colony that does not appear clearly in the early stages, because the diffusion of signaling molecules is spatially limited and significantly slower than the kinetic dynamics of bacteria. Figure 6a shows the evolution of the AHL amount inside cells over time. It shows the mean and variance of 20 independent runs of the simulation. Indeed, from the beginning of the simulation to $\mathrm{t} \simeq 180\ \mathrm{min}$, the AHL amount was stable, but after this crucial moment, at which the quorum is reached, the intracellular AHL amount begins to accelerate exponentially up to 0.6. In our model, unlike the seminal work of (Melke et al., 2010), the AHL does

Figure 4. Bacteria network links and nodes. (a) WT-cooperator bacteria can connect to cooperators and cheaters. (b) Cooperator bacteria can connect to cheaters and can receive signals from WT-cooperators. (c) A cheater cannot connect to WT-cooperators and cooperators, but can receive signals. As a cell accumulates gfp, it can switch to the other cell type. Cheaters can switch to be cooperators and cooperators can switch to be WT-cooperators.

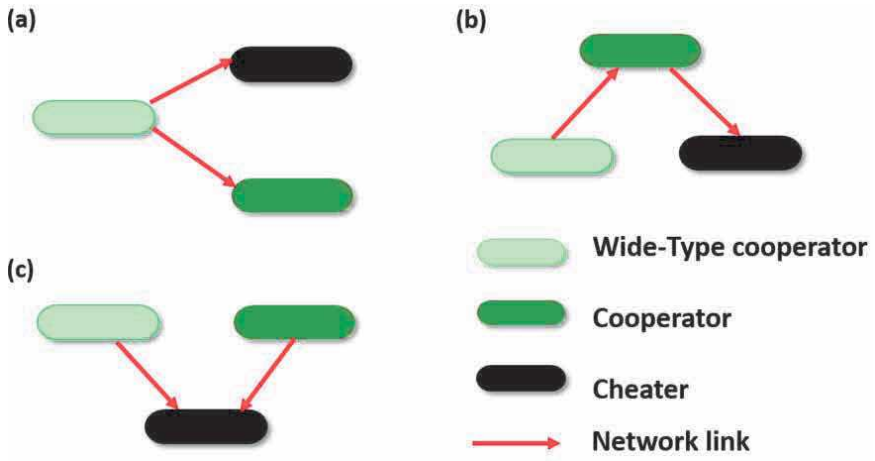

Figure 5. Evolution of bioluminescence. Substrate is shown in purple, AHL in blue, black cells are non-fluorescent. Fluorescence is expressed as a gradient ranging from dark to light green. (a), (b) and (c) represent the beginning of the simulation: cells grow and divide. In (d), (e), the quorum is being reached, fluorescent cells begin to appear. Finally, (f), (g) and (h) show homogenous behavior of bioluminescent cells.

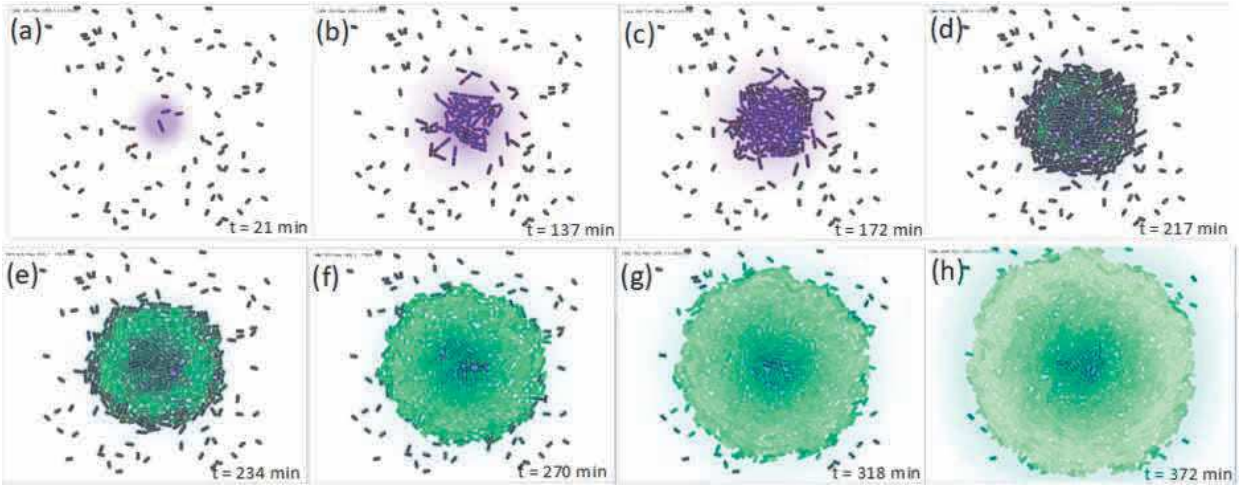

Figure 6. Intracellular molecular dynamics: mean and variance of 20 independent runs. (a) Evolution of autoinducer *A*. (b) Evolution of the dimerized complex *C*. (c) Evolution of bioluminescence gfp/*volume*. (d) Evolution of the number of bioluminescent cells.

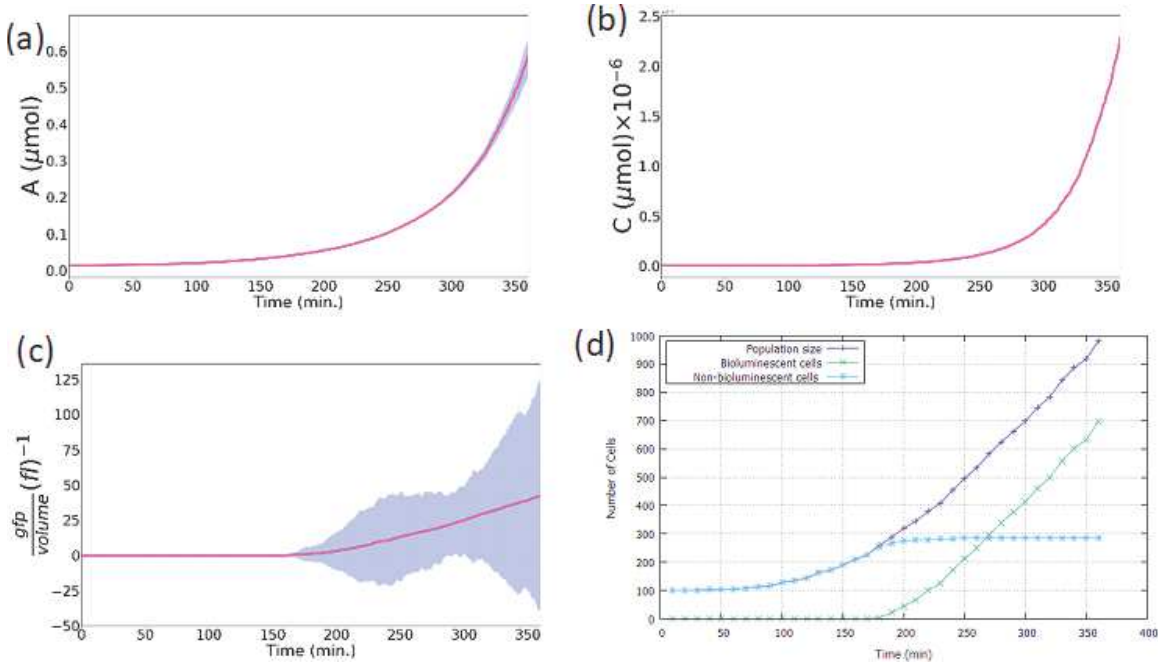

not exist abandonment in the environment (no initialization of substrate in the environment), but it is rather only produced and realized by cells. However, in our simulations the AHL level exceeds the rate achieved in (Melke et al., 2010) (0.6 against 0.1). This shows that the cells in our model provide a stable self-sustainable behavior that allows them to exploit the metabolism to grow, reproduce, survive, and thus produce more AHL molecules, which in turn triggers communication.

Bioluminescence

Bioluminescence is shown as a gradient ranging from dark to light green. In Figure 5, green cells are bioluminescent cells while black cells are not bioluminescent. It is interesting to understand the

bioluminescence regulation at the molecular level. Indeed, at high cell densities, the number of cells exceeding 250 contributes to the increase of AHL emitted by all the cells in the environment. This accelerates exponentially the production rates of AHL by cells, thanks to the positive feedback loop in Equation 1. Consequently, the intracellular amount of the dimerized complex C increases as well, which can be seen in Figure 6b, where the quantity of the dimerized complex begins to increase exponentially from $t \simeq 180\ min$. At this point, the values of the light production rate given by Equation 12 are non-null, and thus cells can accumulate gfps and express bioluminescence. Bioluminescence is observed from $\mathrm{t} = 217\ \mathrm{min}$ in Figure 5d.

Figure 6c presents the evolution of the mean and variance of the gfp amount inside cells. It shows that cells begin to produce gfp from $\mathrm{t} \simeq 180\ \mathrm{min}$, when the quorum is met. It also shows a high variance in the gfp values. Indeed, cells show different light intensities *i.e.* different shades of green that can also be observed in Figure 5. This is called phenotypic heterogeneity. Indeed, real populations of bacteria show that the bioluminescence strength varies throughout the glowing cells (Anetzberger et al., 2012; González-Cabaleiro, Mitchell, Smith, Wipat, & Ofiţeru, 2017; Grote, Krysciak, & Streit, 2015).

It is interesting to observe the bioluminescence behavior at individual and population level. At the individual level, the number of bioluminescent cells represents 73% of the population (see Figure 6d). This corresponds to the empirical rates found in real populations of bacteria. In fact, analysis of the QS-regulated bioluminescence of a wild type strain revealed that, even at high cell densities, only 69% of the cells of the population produced bioluminescence, 25% remained dark and 6% were dead (Anetzberger, Pirch, & Jung, 2009; Pérez & Hagen, 2010).

At the beginning of the simulation, in Figure 5a-f, the arrangement of bioluminescent cells is not homogeneous, and we cannot observe a spatial self-organized behavior at the population level. Towards the end of the simulation, starting at t= 318 min, we can clearly see the degradation of the fluorescence from the center of the colony towards the extremities. Bioluminescent cells organize themselves around the colony to locate at its edges.

Metabolism Evolution

Figure 7 shows the evolution of the cell metabolism via the ATP curve which can be divided into four periods. At the beginning of the simulation (t = 0), the ATP level was equal to the basal level. Then, from t = 0 to 25 min, the more cells take up substrates, the more their ATP level starts having values higher than the basal level to stabilizes on between 104 and 107 units average.

Figure 7. Evolution of *ATP*

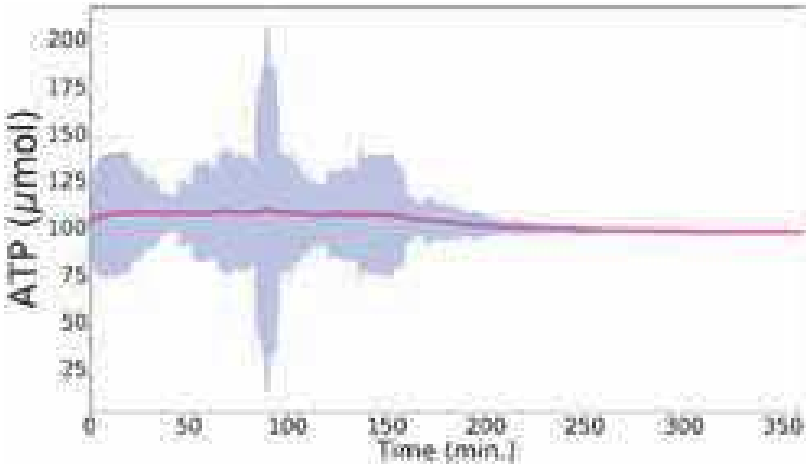

Once the quorum is met at $t \simeq 180\ min$ and the cells begin to produce gfp, the ATP rate starts decelerate. This is due to the energy cost of bioluminescence. From t = 250 min to the end of the simulation, the ATP level stabilizes, which provides a stable self-sustainable behavior.

Consequently, the different runs show that the QS has a positive influence on the cells energy regulation. In fact, actual populations of bacteria show that QS induces a series of extracellular factors that promote population growth and energy regulation (Popat et al., 2015; Schuster, Joseph Sexton, Diggle, & Peter Greenberg, 2013; P. Williams, Winzer, Chan, & Cámara, 2007).

Network Evolution

A cell is considered to be sensitive to light if its intracellular concentration of $luxR$ is above a threshold $T\_R = 0,0155$. The first network measure we calculate, is the number of cells of each of the node type. This is represented in Figure 8a. From t = 0 to t = 50 min, the number of cheaters is stable and equal to 50 cells. After this, the number of cheaters begins to increase gradually, when it reaches its maximum i.e. 294 cells at t = 260 min. Then, this number stagnates until the end of the simulation. At t = 210 min, the quorum is reached, the cells begin to emit light, and consequently cooperator cells begin to appear in the population.

At t = 300 min the number of cooperators exceeds the number of cheaters, while WT-cooperator cells start appearing. The number of cooperators and wild-type cooperators go on increasing as the number of cells increases, while the number of cheaters remains stable. At the end of the simulation, we notice that cooperator cells are dominant in the population with 752 cells which represent 54.89% of the population, against 294 of cheaters and 324 of WT-cooperators which represent respectively 21.46% and 23.65% of the population.

The second measure we calculated is the number of links. This is represented in Figure 8b. From $t = 230 - 350 min$, the total number of links is minimal. This number explodes at $t = 350$, when the

Figure 8. Evolution of the network properties. (a) Evolution of the number of nodes. (b) Evolution of the number of links. (c) Evolution of the number of networked nodes.

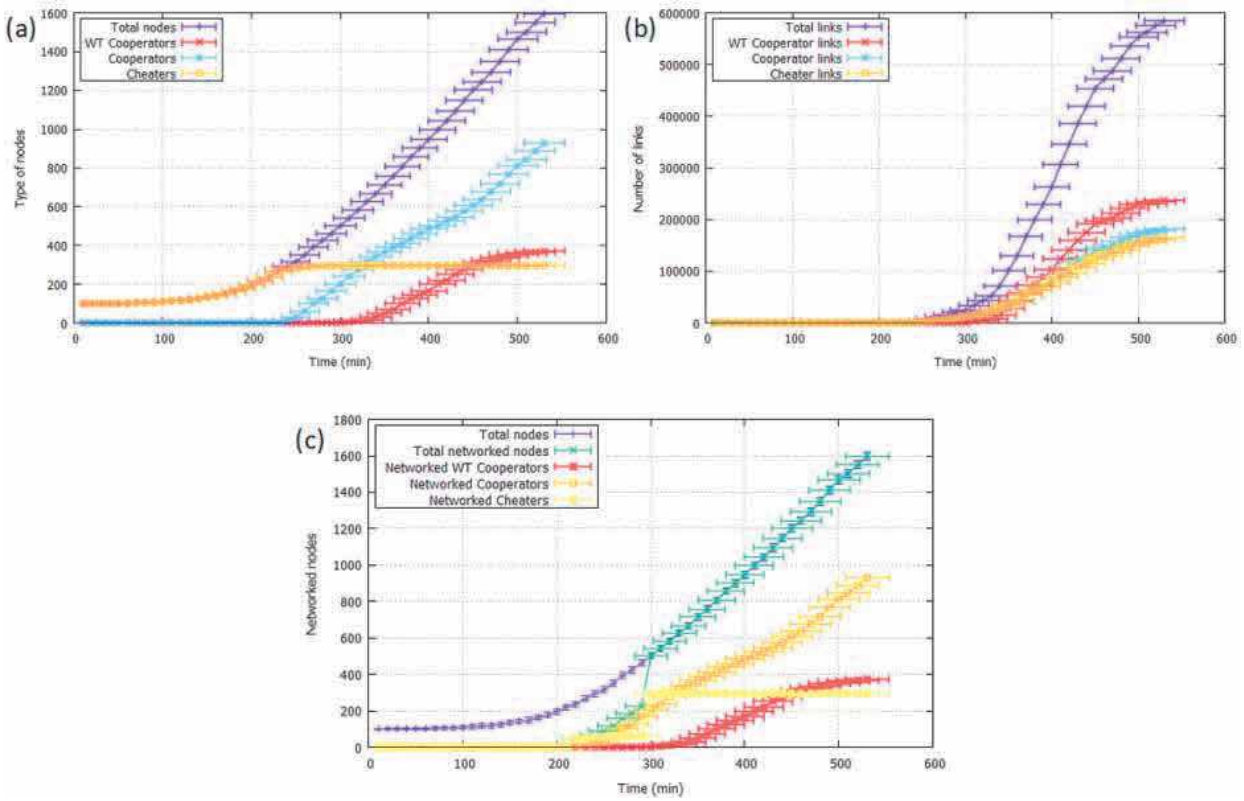

number of cooperator links takes over. At the end of the simulation, it can be clearly seen that despite the fact that the number of WT-cooperators does not exceed 23.65%, the number of links of Wild-type cooperators cells largely exceeds that of the other cell types with 41.12% of all links versus 27.93% of cheater links and 30.94% of cooperators links. Another very important point to emphasize, is that despite the number of cheaters stagnated from $t = 260 min$, the number of cheater links goes on increasing which means that these cells continue to receive links in order to be connected to the entire population.

Figure 8c represents the third measure we calculated, the number of networked cells. At $t = 290 min$, networked WT-cooperator cells begin to emerge, and the number of networked cells fit the total number of total cells (the number of non-networked cells is equal to 0). This means that, WT cooperators cells have a high degree of cooperation and allow the entire population to be connected. In order to explore this observation further, in the next section we measure the cooperation degree to observe how cooperation evolves through the simulations.

Cooperation and Coercion

Thought the study of cooperation has preoccupied researchers for centuries, the potential for social behavior in microbiomes has only recently been recognized (Tarnita, 2017). Indeed, as in societies at the macroscopic scale, within microbiomes, different types of bacteria tend to coexist in conflict or in cooperation for common interests. Since our model uses cooperation expressed via light, as a basis underlying cooperative artificial network formation, we consider:

1. The number of cooperators (respectively WT cooperators) as a cost; and
2. The resulting network components: total links and networked nodes as benefits, which we call common interests.

Then, we calculate cooperation as the benefit/cost ratio. So that, the benefit/cost ratio expresses to what extent cooperators contribute to the evolution of the common interest. In this experiment we consider two common interests. The first common interest represents the total number of links. The second the number of networked cells.

Figure 9a shows the evolution of cooperation toward common interest 1. At t = 300 min, the cooperation level of WT cooperators reaches its peak, while the cooperator's one is equal to zero. This situation changes progressively from t =310-380 min. Indeed, the cooperation level of WT cooperators starts decreasing while that of cooperators begins to show positive values. In this case, WT cooperators seem to show a kind of "coercive" behavior, as they force (coerce) cooperators to change their behavior. Their level of cooperation shifts from zero to positive values, i.e. WT cooperators coerce the other variant to cooperate.

We consider this behavior, which has not been predicted in the model design, as an "emerging" coercive strategy. A strategy is termed coercive if the production of substance X by cell A forces a clear response from cell B (Diggle, Gardner, West, & Griffin, 2007).

Initially, from t = 300-380 min, WT cooperators "coerce" other individuals (i.e. cooperators) to produce more links, while producing less themselves (see also Figure 8b at t = 300-380 min). The initial increase in the cooperation level of WT cooperators is due to the benefits of their coercive strategy (high signalers, low producers of links) in presence of other cooperator variants i.e. cooperators (low signalers, high producers of links), however, as the cooperator's cooperation starts increasing the diminishing levels of the WT cooperator cooperation ultimately makes coercive strategy much moderates from t= 380 min. This behavior will stabilize until the end of the simulation.

Figure 9b shows the evolution of the cooperation degree toward the common interest 2: networked cells. Similarly, a coercion behavior is observed at t = 300. Cooperation levels of the two variants stabilize from t= 400 min and remain stable until the end of the simulation. Final values are summarized in Table 1.

As a global statement, it is important to note that, at any time, the cooperation degree of WT cooperator toward both common interests (Figure 9a and 9b) is higher than that of cooperators.

Figure 9. Evolution of cooperation. (a) Evolution of cooperation toward the common interest 1: total links. (b) Evolution of cooperation toward the common interest 2: networked cells.

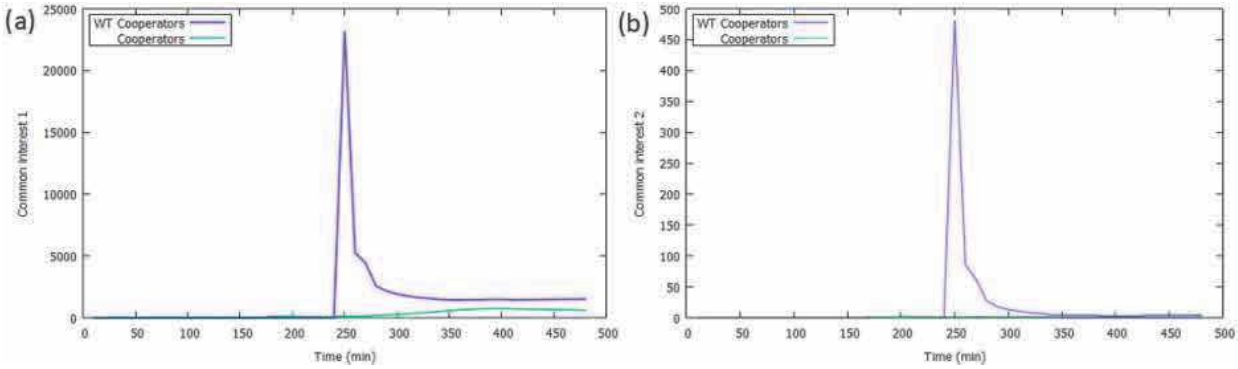

Table 1. Final values of cooperation toward common interests

	WT Cooperators	Cooperators
Common interste1	1514	613
Common interest 2	4	1

Consequently, up-regulated cells, here WT cooperators, have a higher degree of cooperation in the evolution of the properties of the subsequent communication network: links and nodes.

DISCUSSION

Results are discussed in two subsections namely: cellular model and artificial network.

Cellular Model

Realistic simulations should involve a large number of bacteria. Our model enables the simulation of growing colonies having up to 2000 bacteria cells while, in the seminal work presented in (Melke et al., 2010), the population size does not exceed 256 cells. Our proposed computational model of bioluminescence is based on a simplification of nature. Nevertheless, bioluminescence emerges as a spontaneous property of the regulation system, without any centralized control on the QS genetic circuit. We note that no cell density counter is used to control QS molecular triggering, and neither global nor local control is exercised on cells and their actions. In (Ouannes et al., 2016), the authors propose an algorithm of QS that uses a cell density counter, to decide the cells behavior. Conversely, in our model, cell actions are executed autonomously by the bacterial agent, all the time and in parallel– just like reactions in real cells are going all the time in parallel.

In most artificial life models, metabolism is rarely taken into account, or it is considerably abstracted into a simplistic one that uses an energy counter, decremented at each time step, as in (Forrest & Jones, 1993; Ouannes et al., 2016; Ouannes, Djedi, Luga, & Duthen, 2014). In such models, there is no real transformation of matter from nutrients to biomass, or ATP. Instead, in our model, there is an actual simulation of such an energy production and consumption. Positive terms in the metabolism equation (Equation 13) describe energy production (transformation of matter i.e. metabolization of substrate into ATP and biomass), while negative terms describe energy consumption. Our work is among the rare works in artificial life that links metabolism to QS, while metabolism control is a kind of QS regulation (Queck et al., 2008; Schuster et al., 2013; Williams et al., 2007). Results show clearly that the ATP curve stabilizes after the quorum is being met.

Artificial Network

Although our communication network is defined on the basis of two simple rules: an emission rule and a reception rule, the network allows the totality of the cells of the population (100%) to be networked, whatever their position (near or far from the colony); their type (QS or non-QS cell, bioluminescent or non-bioluminescent cell). We note that the results converged as a spontaneous evolution of the network dynamics without the use of any evolutionary algorithm. Because unicellular organisms are autonomous, the network developed by these unicellular organisms is autonomous too. Moreover, the network links are established upon communication rules that respect the simple bacteria policy of communication. This is challenging for the morphogenesis of autonomous network topologies that can be developed in the future. Indeed, the emergent communication networks establish links, in a cooperative manner, upon reproductive and self-energy producer nodes (metabolism).

Coercive Strategy

Currently, a lot of works tend to investigate coercive strategies in microbial societies to answer various questions, for example, to ask whether QS within bacteria is a honest signaling, or whether QS is also used for the coercion of other cells (Allen, McNally, Popat, & Brown, 2016; Diggle et al., 2007; Popat, Cornforth, McNally, & Brown, 2014; Roman Popat et al., 2015). In our simulated microbial society, WT cooperators coerced other individuals to cooperate. This coercive strategy has been shown to be beneficial to share the common interests between two variants of cooperators, otherwise, the system might be invaded by a variant of cooperators that do not cooperate to common interests.

The problem of honesty arises when individuals signal dishonestly to coerce others into behaving in a way that benefits the signaler, prompting the question of what maintains signal honesty (Dawkins, 1978)? Evolutionary theory has suggested that honesty can be maintained through mechanisms such as a common interest between signaler and receiver (Searcy & Nowicki, 2005). Results show that our model behaves with respect to this suggestion i.e. honest signaling is maintained to coerce other individuals to cooperate for common interests.

Note that the social behavior of microorganisms, with respect to evolutionary theory, has been studied only recently (Crespi, 2001), and researchers recognize that there is a great potential for interdisciplinary research to explore this area from different perspectives (Asfahl & Dandekar, 2018; Tarnita, 2017; West, Griffin, Gardner, & Diggle, 2006).

CONCLUSION

The novelty of the paper is that the simulation model considers some key biological processes such as growth, quorum sensing, bioluminescence and metabolism. Moreover, in this paper, local intra and intercellular dynamics at the level of a cell bimolecular interactions are abstracted into a global communication system. This leads to the emergence of homogenous behaviors over the population, e.g. the cooperation to common interests in the evolution of the light-based communication networks. This cooperation allows the total of the cells of the population to be networked.

Not only this paper expands the scope of QS in the field of artificial life systems, it also provides more evidence that QS bacteria relying on AHL as signaling molecules should not be under-estimated. Indeed, results show that the evolution of cooperation leads to the emergence of coercive strategies which have not been predicted in the model design. Coercive strategy has been shown to be beneficial to share the common interests between two variants of cooperators, otherwise the system could be invaded by a variant of cooperators who do not cooperate to common interests.

We hope that our models of metabolism and bioluminescence may inspire researchers to develop new bioinspired computational models, where multiple distributed, autonomous and energy-producing agents need to coordinate their behavior efficiently, based on very limited local information of their environment, to exhibit interesting behaviors at the population level.

As future works, the network model could be extended further. For example, since we are using gfp, green fluorescent proteins, we could also establish different light emissions: red, yellow or green

lights. To do so, we could add components to the genetic circuit such as photosensitive promoters, e.g. different promoters for different light wavelengths: green, red, yellow. Moreover, the network could also be evolved with an evolutionary algorithm to solve specific problems such as optimizing energy.

MODEL PARAMETERS

Table 2 lists the parameters used in our model. The values of some parameters have been experimentally tuned, for example, to allow to visualize graphically certain behaviors e.g. L_{max}, or to prolong the

Table 2. Model parameters

Parameter	Value	Unit
C_A, C_R	1e-4	μM
k_A, k_R	2e-3	-
K_A, K_R	1e-9	μM
k_0, k_3	1e-2	-
k_1, k_2, k_4, k_5	1e-1	-
p_e	*0.025*	-
p_a	*0.025*	-
μ_{max}	*0.034*	*fl/min*
K_S	*1*	μMol
$Y_{X/ATP}$	0.034	$fl \ / \ \mu Mol$
L_{max}	2e-1	$RLU \ / \ min$
K_L	2.1e-7	μMol
ATP_0	*1000*	μMol
$Y_{ATP/S}$	1000	-
$Y_{L/ATP}$	0.135	$RLU \ / \ \mu Mol$
T_L	0.20	-

cell survival e.g. $\left(ATP_0\right)$. QS parameters are adopted from a $LuxIR$ system (Melke et al., 2010). Other parameters are variable, and are described in the main body of this document. We assume that the light intensity units are proportional to Relative Light Units (RLU).

REFERENCES

Amir, Y., Abu-Horowitz, A., Werfel, J., & Bachelet, I. (2018). Nanoscale robots exhibiting quorum sensing. doi:10.1101/448761

Anetzberger, C., Pirch, T., & Jung, K. (2009). Heterogeneity in quorum sensing-regulated bioluminescence of Vibrio harveyi. *Molecular Microbiology*, *73*(2), 267–277. doi:10.1111/j.1365-2958.2009.06768.x PMID:19555459

Anetzberger, C., Reiger, M., Fekete, A., Schell, U., Stambrau, N., Plener, L., & Jung, K. et al. (2012). Autoinducers Act as Biological Timers in Vibrio harveyi. *PLoS One*, *7*(10), e48310. doi:10.1371/journal.pone.0048310 PMID:23110227

Asfahl, K. L., & Dandekar, A. A. (2018). Social Evolution: Selection on Multiple Cooperative Traits Optimizes Cost–Benefit Relationships. *Current Biology*, *28*(13), R752–R755. doi:10.1016/j.cub.2018.05.034 PMID:29990460

Aziz, A. A., Sekercioglu, Y. A., Fitzpatrick, P., & Ivanovich, M. (2013). A Survey on Distributed Topology Control Techniques for Extending the Lifetime of Battery Powered Wireless Sensor Networks. *IEEE Communications Surveys and Tutorials*, *15*(1), 121–144. doi:10.1109/SURV.2012.031612.00124

Bassler, B. L. (1999). How bacterial talk to each other: Regulation of gene expression by quorum sensing. *Current Opinion in Microbiology*, *2*(6), 582–587. doi:10.1016/S1369-5274(99)00025-9 PMID:10607620

Bechon, P., & Slotine, J.-J. (2012). Synchronization and quorum sensing in a swarm of humanoid robots.

Beckmann, B. E., & Mckinley, P. K. (2009). Evolving Quorum Sensing in Digital Organisms. In *GECCO '09 Proceedings of the 11th Annual conference on Genetic and evolutionary computation* (pp. 97–104). Academic Press. doi:10.1145/1569901.1569916

Burgos, A. C., & Polani, D. (2016). Cooperation and antagonism in information exchange in a growth scenario with two species. *Journal of Theoretical Biology*, *399*, 117–133. doi:10.1016/j.jtbi.2016.04.006 PMID:27071539

Callaway, E. (2013). Glowing plants spark debate. *Nature*, *498*(7452), 15–16. PMID:23739402

Dawkins, R. (1978). Animal signals: information or manipulation. In J. R. Davies & K. and N. B. (Eds.), Behavioural ecology: An evolutionary approach (pp. 282-309). Oxford, UK: Blackwell Scientific Publications.

Djezzar, N., Fernandez Perez, I., Djedi, N., & Duthen, Y. (n.d.). Digital Simulation of Bioluminescent Bacteria Cells Tweeting via Quorum-Sensing Molecules. In T. Ikegami, N. Virgo, & O. Witkowski (Eds.), *Artificial Life, Tokyo* (p. L19). Tokyo: MIT Press. Retrieved from http://mitpress.mit.edu/

Doursat, R., Sayama, H., & Michel, O. (2013). A review of morphogenetic engineering. *Natural Computing*, *12*(4), 517–535. doi:10.1007/s11047-013-9398-1

Dressler, F., & Akan, O. B. (2010). A survey on bio-inspired networking. *Computer Networks*, *54*(6), 881–900. doi:10.1016/j.comnet.2009.10.024

Emerenini, B. O., Hense, B. A., Kuttler, C., & Eberl, H. J. (2015). A Mathematical Model of Quorum Sensing Induced Biofilm Detachment. *PLoS One*, *10*(7), e0132385. doi:10.1371/journal.pone.0132385 PMID:26197231

Esmaeili, A., & Yazdanbod, I. (2009). A Model of the Quorum Sensing System In Genetically Engineered E. Coli Using Membrane Computing. In *International Genetic Engineered Machines Competition (IGEM)*. Academic Press. Retrieved from https://pdfs.semanticscholar.org/f6cf/b43c1ad77390ccf60678bbf6225f895be7e1.pdf

Forrest, S., & Jones, T. (1994). Modeling complex adaptive systems with Echo. *Complex systems: Mechanisms of adaptation*, 3-21.

González-Cabaleiro, R., Mitchell, A. M., Smith, W., Wipat, A., & Ofiţeru, I. D. (2017). Heterogeneity in Pure Microbial Systems: Experimental Measurements and Modeling. *Frontiers in Microbiology*, *8*, 1813. doi:10.3389/fmicb.2017.01813 PMID:28970826

Gorochowski, T. E. (2016). Agent-based modelling in synthetic biology. *Essays in Biochemistry*, *60*(4), 325–336. doi:10.1042/EBC20160037 PMID:27903820

Grote, J., Krysciak, D., & Streit, W. R. (2015). Phenotypic Heterogeneity, a Phenomenon That May Explain Why Quorum Sensing Does Not Always Result in Truly Homogenous Cell Behavior. *Applied and Environmental Microbiology*, *81*(16), 5280–5289. doi:10.1128/AEM.00900-15 PMID:26025903

Jang, S. S., Oishi, K. T., Egbert, R. G., & Klavins, E. (2012). Specification and Simulation of Synthetic Multicelled Behaviors. *ACS Synthetic Biology*, *1*(8), 365–374. doi:10.1021/sb300034m PMID:23651290

Ji, W., Shi, H., Zhang, H., Sun, R., Xi, J., Wen, D., & Ouyang, Q. et al. (2013). A Formalized Design Process for Bacterial Consortia That Perform Logic Computing. *PLoS One*, *8*(2), e57482. doi:10.1371/journal.pone.0057482 PMID:23468999

Majumdar, S., & Mondal, S. (2016). Conversation game: Talking bacteria. *Journal of Cell Communication and Signaling*, *10*(4), 331–335. doi:10.1007/s12079-016-0333-y PMID:27278085

Melke, P., Sahlin, P., Levchenko, A., & Jönsson, H. (2010). A cell-based model for quorum sensing in heterogeneous bacterial colonies. *PLoS Computational Biology*, *6*(6), e1000819. doi:10.1371/journal.pcbi.1000819 PMID:20585545

Monod, J. (1949). The Growth of Bacterial Cultures. *Annual Review of Microbiology*, *3*(1), 371–394. doi:10.1146/annurev.mi.03.100149.002103

Moreno-Fenoll, C., Cavaliere, M., Martínez-García, E., & Poyatos, J. F. (2017). Eco-evolutionary feedbacks can rescue cooperation in microbial populations. *Scientific Reports*, *7*(1), 42561. doi:10.1038/srep42561 PMID:28211914

Niu, B., Wang, H., Duan, Q., & Li, L. (2013). Biomimicry of quorum sensing using bacterial lifecycle model. *BMC Bioinformatics*, *14*(Suppl 8), S8. doi:10.1186/1471-2105-14-S8-S8 PMID:23815296

Ouannes, N., Djedi, N., Duthen, Y., & Luga, H. (2016). *Emergent group behaviors from bacteria quorum sensing simulation. In 21st AROB* (pp. 62–67)., Retrieved from https://www.researchgate.net/profile/Noureddine_ Djedi/publication/292145144_Emergent_group_behaviors_from_bacteria_quorum_sensing_simulation/links/56aa4cc108aef6e05df45c2f/Emergent-group-behaviors-from-bacteria-quorum-sensing-simulation.pdf

Ouannes, N., Djedi, N., Luga, H., & Duthen, Y. (2014). Modeling a bacterial ecosystem through chemotaxis simulation of a single cell. *Artificial Life and Robotics*, *19*(4), 382–387. doi:10.1007/s10015-014-0187-4

Pascalie, J., Potier, M., Kowaliw, T., Giavitto, J.-L., Michel, O., Spicher, A., & Doursat, R. (2016). Developmental Design of Synthetic Bacterial Architectures by Morphogenetic Engineering. *ACS Synthetic Biology*, *5*(8), 842–861. doi:10.1021/acssynbio.5b00246 PMID:27244532

Pérez, P. D., & Hagen, S. J. (2010). Heterogeneous Response to a Quorum-Sensing Signal in the Luminescence of Individual Vibrio fischeri. *PLoS One*, *5*(11), e15473. doi:10.1371/journal.pone.0015473 PMID:21103327

Popat, R., Pollitt, E. J. G., Harrison, F., Naghra, H., Hong, K., Chan, K., & Diggle, S. P. et al. (2015). Conflict of interest and signal interference lead to the breakdown of honest signaling. *Evolution*, *69*(9), 2371–2383. doi:10.1111/evo.12751 PMID:26282874

Queck, S. Y., Jameson-lee, M., Villaruz, A. E., Bach, T. L., Burhan, A., Sturdevant, D. E., & Otto, M. et al. (2008). RNAIII-independent target gene control by the agr quorum-sensing system: Insight into the evolution of virulence regulation in Staphylococcus aureus. *Molecular Cell*, *32*(1), 150–158. doi:10.1016/j.molcel.2008.08.005 PMID:18851841

Romero-Campero, F. J., & Pérez-Jiménez, M. J. (2008). A Model of the Quorum Sensing System in *Vibrio fischeri* Using P Systems. *Artificial Life*, *14*(1), 95–109. doi:10.1162/artl.2008.14.1.95 PMID:18171133

Schuster, M., Joseph Sexton, D., Diggle, S. P., & Peter Greenberg, E. (2013). Acyl-Homoserine Lactone Quorum Sensing: From Evolution to Application. *Annual Review of Microbiology*, *67*(1), 43–63. doi:10.1146/annurev-micro-092412-155635 PMID:23682605

Searcy, W. A., & Nowicki, S. (2005). *The evolution of animal communication : reliability and deception in signaling systems*. Princeton University Press. Retrieved from https://press.princeton.edu/titles/8110.html

Sexton, D. J., & Schuster, M. (2017). Nutrient limitation determines the fitness of cheaters in bacterial siderophore cooperation. *Nature Communications*, *8*(1), 230. doi:10.1038/s41467-017-00222-2 PMID:28794499

Sofge, D. A., & Lawless, W. F. (2011). Quorum Sensing for Collective Action and Decision-Making in Mobile Autonomous Teams. In ICAART (Vol. 1, pp. 195–204). Academic Press. doi:<ALIGNMENT.qj></ALIGNMENT>10.5220/0003122501950204

Song, S., & Yamada, S. (2018). Bioluminescence-Inspired Human-Robot Interaction. In *Proceedings of the 2018 ACM/IEEE International Conference on Human-Robot Interaction - HRI '18* (pp. 224–232). New York, NY: ACM Press. doi:10.1145/3171221.3171249

Stanley, K. O., & Miikkulainen, R. (2003). A Taxonomy for Artificial Embryogeny. *Artificial Life*, *9*(2), 93–130. doi:10.1162/106454603322221487 PMID:12906725

Tan, F., & Slotine, J.-J. (2013). A Quorum Sensing Inspired Algorithm for Dynamic Clustering. In *Proceedings of the 2013 IEEE 52nd Annual Conference on Decision and Control (CDC), (pp. 5364-5370* (pp. 5364–5370). IEEE. Retrieved from http://arxiv.org/abs/1303.3934

Tarnita, C. E. (2017). The ecology and evolution of social behavior in microbes. *The Journal of Experimental Biology*, *220*(Pt 1), 18–24. doi:10.1242/jeb.145631 PMID:28057824

Wei, G., Walsh, C., Cazan, I., & Marculescu, R. (2015). Molecular tweeting: Unveiling the social network behind heterogeneous bacteria populations. In *BCB 2015 - 6th ACM Conference on Bioinformatics, Computational Biology, and Health Informatics* (pp. 366–375). ACM. doi:10.1145/2808719.2808757

West, S. A., Griffin, A. S., Gardner, A., & Diggle, S. P. (2006). Social evolution theory for microorganisms. *Nature Reviews. Microbiology*, *4*(8), 597–607. doi:10.1038/nrmicro1461 PMID:16845430

Wiedermann, J. (2011). Nanomachine computing by quorum sensing. In *Computation, cooperation, and life* (pp. 203–215). Springer; doi:10.1007/978-3-642-20000-7_17

Williams, J. W., Cui, X., Levchenko, A., & Stevens, A. M. (2008). Robust and sensitive control of a quorum-sensing circuit by two interlocked feedback loops. *Molecular Systems Biology*, *4*(1), 234. doi:10.1038/msb.2008.70 PMID:19096361

Williams, P., Winzer, K., Chan, W. C., & Cámara, M. (2007). Look who's talking: Communication and quorum sensing in the bacterial world. *Philosophical Transactions of the Royal Society of London. Series B, Biological Sciences*, *362*(1483), 1119–1134. doi:10.1098/rstb.2007.2039 PMID:17360280

Zeng, A.-P., & Deckwer, W.-D. (1995). A kinetic model for substrate and energy consumption of microbial growth under substrate-sufficient conditions. *Biotechnology Progress*, *11*(1), 71–79. doi:10.1021/bp00031a010 PMID:7765990

Zhao, J., & Wang, Q. (2017). Three-Dimensional Numerical Simulations of Biofilm Dynamics with Quorum Sensing in a Flow Cell. *Bulletin of Mathematical Biology*, *79*(4), 884–919. doi:10.1007/s11538-017-0259-4 PMID:28290008

Zhao, Q., Li, M., Wang, Z., Li, J., & Luo, J. (2015). A Quorum Sensing algorithm to control nanorobot population and drug concentration in cancer area. In *Proceedings of the 2015 IEEE International Conference on Robotics and Biomimetics (ROBIO)* (pp. 42–47). IEEE. doi:10.1109/ROBIO.2015.7407037

Nedjma Djezzar is an assistant professor at the Computer Science department of Batna University (Algeria) and a member of ReVa team at IRIT lab, Toulouse (France). She is also a Ph.D. Student at the University of Toulouse Capitole (France) and University of Biskra (Algeria). In 2007, she obtained her state engineer degree in Advanced Information Systems with Honors at the University of Constantine. In 2010, she obtained her Magister degree with High Honours in Image Synthesis and Artificial Life, at the University of Biskra. She has published 4 refereed conference papers. Her research interests include artificial life, morphogenetic engineering, nature inspired computing, and complex adaptive systems modeling.

Iñaki Fernández Pérez obtained his B.Sc. in Computer Systems at the University of Valladolid, Spain, in 2010. In 2013, he obtained his M.Sc. in Artificial Intelligence at the University of Lorraine, Nancy, France, with a thesis in Evolutionary Robotics. In 2017, he received his Ph.D. degree in adaptation in robot swarms. Currently, he is a postdoctoral fellow within the ReVa team at the University of Toulouse, France, and his research interests include adaptive collective systems, artificial life, machine learning, swarm robotics, evolutionary computation and neuroevolution.

Noureddine Djedi received a B.Sc. degree in Computer Science from USTHB University in Algeria in 1986. He received his M.Sc. and Ph.D. degrees in computer graphics from Paul Sabatier University (Toulouse III) France. in 1987 and 1991, respectively. He was the head of LESIA Laboratory from 2008 to 2011. He has published about 80 refereed journal and conference papers. His research interests include robotics, image synthesis, artificial life, and behavioral animation.

Yves Duthen is a Research Professor of Artificial Life and Virtual Reality at IRIT lab, University of Toulouse 1-Capitole (France). He received his Ph.D. degree from the University Paul Sabatier in 1983 and the "French Habilitation" degree in 1993 to become full Professor. He has worked in image synthesis during the 1980's and focused on Behavioral Simulation based on evolutionary mechanism since 1990. He has published about 130-refereed journal and conference papers and has directed 15 PhD theses. He has pioneered research in artificial life for building adaptive artificial creatures and focuses now on embedded metabolism, and morphogenetic engineering.